Guadilla *et al.*
The Journal of Headache and Pain (2025) 26:31
https://doi.org/10.1186/s10194-025-01970-z

The Journal of Headache and Pain

RESEARCH

Open Access

White matter alterations in episodic migraine without aura patients assessed with diffusion MRI: effect of free water correction

Irene Guadilla[1,2,3*], Ana R Fouto[2], Amparo Ruiz-Tagle[2], Inês Esteves[2], Gina Caetano[2], Nuno A Silva[4], Pedro Vilela[5], Raquel Gil-Gouveia[6,7], Santiago Aja-Fernández[3], Patrícia Figueiredo[2] and Rita G Nunes[2]

Abstract

Objective To assess the effect of modeling free water (FW) on the identification of white matter (WM) microstructure alterations using diffusion Magnetic Resonance Imaging (dMRI) in episodic migraine without aura patients compared with healthy controls.

Background Diffusion tensor imaging (DTI) studies examining WM in migraine patients previously overlooked the potential influence of FW partial volume effects. Correcting FW effects could offer a clearer understanding of WM changes in migraine. This study is the first to incorporate FW effects when evaluating alterations in WM tracts in migraine patients, offering a comparison to standard DTI analysis.

Methods A group of 14 patients with low-frequency episodic menstrual-related migraine without aura and 15 healthy controls matched for the phase of the menstrual cycle were recruited and underwent dMRI acquisitions. FW partial volume fraction was estimated, the diffusion signal corrected and the diffusion parameters calculated from both FW-corrected and uncorrected signals. Tract-Based Spatial Statistics (TBSS) and WM skeleton regions of interest (ROI) analyses were used to compare between groups.

Results Comparisons between control subjects and migraine patients with TBSS and ROI analyses revealed significantly lower axial diffusivity (AD), both with and without FW correction, as well as altered FW values in migraine patients in some WM tracts. TBSS detected MD changes only after FW correction.

Conclusions These findings suggest WM alterations in these migraine patients in comparison with control subjects, in accordance with other migraine studies. Differences in the diffusion parameters might point to inflammatory processes in migraine related to cellular swelling.

Keywords Episodic migraine, Menstrual-related migraine, Microstructure, White matter, Diffusion tensor imaging, Free water

*Correspondence:
Irene Guadilla
irene.guadilla@uva.es
Full list of author information is available at the end of the article

Background

Migraine affects over 15% of the global population, being one of the most common and disabling neurological disorders [1]. Migraine is characterized by recurrent episodes of headaches accompanied by symptoms such as photophobia or nausea. Its prevalence varies by sex and age, affecting women three times more than men, especially during the reproductive years. Among the different types of migraine [2], migraine without aura is by far the most common. One type - menstrual-related migraine - affects nearly a quarter of female migraine patients and exhibits unique features not found in other types of migraine. These subjects experience regular attacks, within two days before menstruation and the first three days of bleeding [3]. Although they can suffer other attacks out of these days (episodic migraine form), menstrual-related migraine attacks usually last longer, are more severe and less responsive to treatment than attacks at other times of the menstrual cycle [4]. Previous studies have indicated that migraine attacks depend on the activation and sensitization of trigeminal sensory afferents [5] and of neurons in brain regions involved in pain response [6]. During migraine attacks, the calcitonin gene-related peptide (CGRP) is released [6]. It is known that CGRP levels can be affected by sex hormones [7, 8] and that receptors for some ovarian hormones, such as estrogen, are located in migraine-related regions, including the trigeminovascular system [8, 9]. Fluctuations in menstrual cycle hormones play an important role in menstrual-related migraine [7], and estrogen withdrawal is currently thought to explain migraine attacks in susceptible women around menses [3].

Several studies have explored brain alterations in migraine patients compared to healthy controls, using magnetic resonance imaging (MRI), positron emission tomography (PET), and single-photon emission computed tomography (SPECT) [10]. Functional MRI revealed alterations in connectivity and activation of pain-processing circuits [11, 12], while structural changes, quantified by the volume of gray matter structures from anatomical T1-weighted MRI scans, have also been reported. Only two studies have focused specifically on brain function and structure in menstrual migraine patients [13, 14], uncovering reduced gray matter volume and increased connectivity in pain-related regions. Another study compared functional brain networks between menstrual and non-menstrual migraine patients, mainly revealing differences in thalamic nodal degree [15]. Additionally, a study distinguished between pure menstrual and menstrual-related migraine patients, highlighting variations in spontaneous neural activity [16].

Diffusion MRI (dMRI) uses water molecular motion to investigate tissue microstructure in various pathological and physiological conditions. Diffusion tensor imaging (DTI), the standard model for analyzing dMRI data, enables the quantification of the following scalar parameters: mean diffusivity (MD), the average water diffusion; axial diffusivity (AD) and radial diffusivity (RD), which measure diffusivity along the main movement direction and directions perpendicular to it, respectively; and fractional anisotropy (FA), which provides information about the anisotropy of diffusion motion [17]. Prior studies employing dMRI have identified white matter (WM) abnormalities in migraine patients, particularly in the corpus callosum (CC), cingulate gyrus (CG), and thalamic radiation [18, 19]. While previous DTI studies showed lower MD values in migraine patients [20, 21], only one dMRI study specifically focused on menstrual-related migraine patients [22], suggesting potential confounding factors in other studies due to patient heterogeneity.

A prior study pointed out that inflammation may play a role in migraine, with altered vascular permeability resulting from a compromised blood-brain barrier [23]. This could impact the extracellular space volume, and such changes would influence the free water (FW) fraction detected in dMRI. The standard DTI description of the dMRI signal can be enhanced using a method called FW-DTI [24], which adds an isotropic high-diffusivity contribution to the mathematical signal description. This extension allows for both the removal of partial volume effects when characterizing WM tissue and the measurement of FW fraction. To enhance specificity in investigating the role of inflammation in migraine, we employed FW-DTI. By isolating FW's contribution from the diffusion signal, this approach improves the specificity of DTI-derived tissue parameters and allows for the evaluation of the FW fraction. Previous studies have suggested that FW fraction may offer insights into biological mechanisms such as neuroinflammation [25] or cognitive impairment [26].

This study examines the effect of FW correction on DTI parameters in investigating WM alterations in episodic menstrual-related migraine patients without aura, compared to controls.

Materials and methods

This study is part of a larger research project on brain imaging in migraine (MigN2Treat), which includes dMRI as well as arterial spin labeling MRI, task-fMRI and resting-state fMRI. In this report, we perform a re-analysis of the dMRI data only. The methods and results for the other analyses are described elsewhere [27–29]. The research protocol and statistical analysis were not preregistered. The study was approved by the Hospital da Luz

Ethics Committee and all participants provided written informed consent according to the Declaration of Helsinki 7th revision.

Participants

The study was performed in low-frequency episodic menstrual-related migraine patients without aura, who were diagnosed according to the International Classification of Headache Disorders [2], with an attack frequency of 2 ± 2.9 per month. A group of female healthy controls was also recruited for comparison. The subjects were distributed as follows: 14 migraine patients (age 36 ± 9 years) and 15 healthy controls (age 31 ± 7 years).

Recruitment was conducted separately for each group but with the same inclusion criteria: (i) age 18 to 55 years; (ii) at least 9 years of education and (iii) native Portuguese. On the other hand, subjects with the following criteria were excluded: (i) neurological medical record (except for migraine in the case of patients); (ii) current psychiatric disorders; (iii) treatment with psychoactive drugs (antidepressants, anticonvulsants), including migraine prophylaxis for the patient group; (iv) contraindications for MRI scanning; and (v) post-menopause, breast-feeding, pregnancy or attempting pregnancy. Patients were recruited from the Neurology Department from Hospital da Luz (Lisbon, Portugal) and the study was conducted in its Imaging Department from 2019 to 2022. Controls were recruited from the general population through an announcement and matched to the clinical sample for age and contraception status.

Study design

Subjects were studied across different sessions, but this report focuses only on one session: migraine patients in the interictal phase (between migraine attacks, pain-free for at least 48 h before the session, and no migraine attack within 72 h after the session) and controls in the respective phase of the menstrual cycle (after ovulation).

MRI data acquisition

Image acquisitions were carried out in a 3T Siemens Vida scanner, with a 64-channel receive radiofrequency coil. Anatomical images (T1-weighted) covering the whole brain were acquired to identify possible brain abnormalities.

dMRI images were collected employing the following parameters: repetition time (TR) = 6800ms, echo time (TE) = 89ms, 8 non-diffusion-weighted images (b = 0s/mm²), b-value = 400, 1000, 2000s/mm², 124 diffusion gradient orientations (32, 32 and 60 directions for each b-value, respectively), 110 × 110 matrix size, spatial resolution of 2 × 2 × 2mm^3 and 66 axial slices covering the entire brain. Additionally, 3 non-diffusion-weighted images with opposite phase encoding (Posterior-Anterior) direction were acquired to enable distortion correction.

MRI data processing and analysis

Diffusion images were preprocessed following the DESIGNER pipeline recommendations [30]. Then, the FW partial volume fraction (Equation S-1) was calculated using the dMRI-Lab toolbox [31] by applying the spherical means (SM) technique to reduce FW estimation bias in crossing fiber regions, using the normalized diffusion signal from b = 400 and 1000s/mm^2. The FW maps were subsequently used to correct the diffusion signal by considering the extended model to remove the FW contribution [32]. DTI parameters (MD, AD, RD and FA) were calculated from the corrected (FW-DTI) and the original (DTI) diffusion signal using DIPY's TensorModel tool [33] in Python (Figure S-1), employing b = 0 and 1000s/mm^2.

Tract-based spatial statistics (TBSS) [34] from FMRIB Software Library (FSL) was used to define a mean WM skeleton. FA data for all subjects, calculated using DTI, were first linearly registered to the FMRIB58 template (voxel resolution of 1 × 1 × 1 mm^3). Next, a non-linear registration procedure was applied to align the FA data of each subject to this common space. A mean FA image was then generated and thinned to create a mean FA skeleton, using an FA threshold of 0.2. The skeleton represents the center of the tracts common to all subjects. The same spatial transformations required to project the individual FA data to the skeleton (affine and non-linear warps) were used to project both the DTI and FW-DTI derived parameters to a common WM skeleton. The WM regions-of-interest (ROI) were identified with the Johns Hopkins University ICBM-DTI-81 WM (JHU-WM) atlas [35], and intersected with the WM skeleton for subsequent ROI analyses.

Statistical analysis

To compare demographic characteristics between groups, we used a two-tailed unpaired t-test.

White matter skeleton comparisons

The diffusion parameters were compared voxelwise using TBSS analysis. We used the *randomise* tool for nonparametric permutation inference to investigate differences between groups, with the threshold-free cluster enhancement option [36], 5000 permutations, and a family-wise error correction for multiple comparisons. Two comparisons were carried out: (i) to test for differences between DTI (original) vs. FW-DTI (corrected) parameters using a paired two-sample t-test for each subject group; (ii) to test for differences in DTI (original) and FW-DTI

Table 1 Clinical and demographic characteristics of control subjects and migraine patients, together with the p-values obtained upon two-tailed unpaired t-tests

	Migraine	Control	*p*-value
n	14	15	
Disease duration (years)	18 ± 10		
Age (years)	36 ± 9	31 ± 7	0.12
Education (years)	16 ± 4	17 ± 1	0.34

(corrected) parameters between migraine patients and controls using an unpaired two-sample t-test. To evaluate the sensitivity of the diffusion parameters estimated from each dMRI model (FW-DTI and simple DTI) when comparing between groups, the percentage of skeleton voxels where significant differences were detected for each diffusion parameter was computed. In the unpaired t-test, the age of the subjects was considered a potential confounding variable in the comparisons between control subjects and migraine patients, and its effect was therefore evaluated.

ROI analysis

WM masks were computed by extracting the corresponding WM skeleton voxels of the 48 ROI included in the JHU-WM atlas. For each region, we calculated the mean value for each subject and diffusion parameters estimated by both methods (DTI and FW-DTI). Subsequently, mean values were compared between groups by employing an analysis of covariance (ANCOVA), considering the age of the subjects as a covariate. The effect size was evaluated using Cohen's d. P-values were adjusted for multiple comparisons using false discovery rate correction. Additionally, we considered statistically significant results only from ROI whose skeleton regions contained over 200 voxels (37 regions) and whose significant voxels summed a volume greater than $50mm^3$. Statistical significance was established at $p < 0.05$.

Results

Demographic characteristics for the migraine ($n = 14$) and control ($n = 15$) groups are shown in Table 1. When comparing age and education years between groups, no statistically significant differences were found.

Diffusion parameters in White Matter

White matter skeleton comparisons: DTI (original) vs. FW-DTI (corrected)

By comparing diffusion parameters across signal models (DTI and FW-DTI), we observed that FW correction consistently resulted in significantly lower MD, AD and RD values, along with higher FA values in the WM tracts across both subject groups. Moreover, we also found that around 98% of the voxels showed significant changes between DTI and FW-DTI parameters (Table S-1) and Figure S-2.

White matter skeleton comparisons: patients vs. controls

TBSS analysis revealed significant differences in WM tracts for MD and AD, with age included as a covariate. Figure 1 highlights regions in the WM skeleton where increased values were observed in diffusion parameters in control subjects compared to patients, for both original DTI and FW-corrected data. Table 2 presents the list of locations where significant changes were detected between the two groups using both signal models (DTI and FW-DTI).

TBSS analysis revealed significantly lower MD values in migraine patients compared to controls (Fig. 1). Our results showed differences between groups in 7 WM tracts only when using the FW-DTI model. These changes were observed in several locations, including the body and splenium of the CC; right retrolenticular part of internal capsule (IC), posterior thalamic radiation (PTR) and superior longitudinal fasciculus (SLF); and left superior corona radiata (CR) and external capsule (EC) (Table 2). Interestingly, significant differences were not detected when the DTI approach was used. However, age had a significant negative effect on the DTI results (MD values decreased with age) in several brain regions from the left hemisphere: anterior and posterior limb and retrolenticular part of the IC, anterior and superior CR, EC and SLF.

Significantly lower AD values were detected in patients (Fig. 1). Our results revealed significant differences in 23 WM tracts regardless of FW correction (Table 2). These WM tracts were mainly located in the left cerebral peduncle (CP) and bilaterally in 7 WM tracts from the projection fibers: IC (anterior and posterior limb, retrolenticular part), CR (anterior, posterior and superior), PTR and SLF. Some association fibers (left sagittal stratum (SS) and bilateral EC) and the CC also exhibited these significant differences. On the other hand, 5 WM tracts presented different statistical results depending on whether FW contamination was removed. The right CP and the left CG and fornix (cres)/stria terminalis (FST) showed significant differences for the AD values estimated from DTI, but not from FW-DTI. Conversely, the AD value from the right SS and cingulum (hippocampus) (CgH) exhibited significant differences with FW-DTI. Additionally, 2 WM tracts from the left hemisphere (posterior limb of IC and anterior CR) presented a negative age effect, meaning that the AD values in those WM tracts significantly decreased with age.

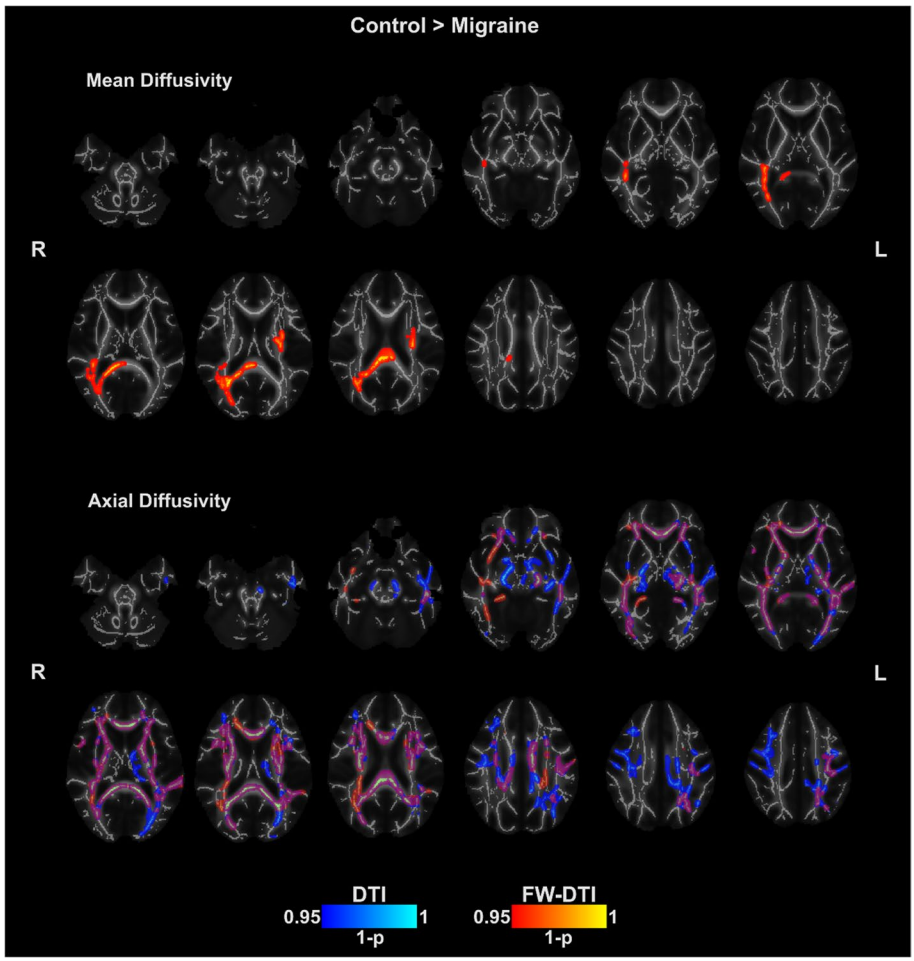

Fig. 1 Locations where statistically significant differences were found in WM tracts in MD (top) and AD (bottom), including age as a covariate. These parametric maps displayed regions of increased values for control subjects compared to patients for both original DTI (blue) and FW-corrected DTI (yellow). Grayscale: FA WM skeleton map (range: 0 to 1). Red-yellow scale (range: 0.95 to 1) represents (1-p)-value for DTI parameters, while blue-light blue scale (range: 0.95 to 1) represents (1-p)-value for FW-DTI parameters. Regions with changes in both DTI and FW-DTI are shown in purple, resulting from the overlap of the color maps. R: right, L: left

Although no significant changes were observed for FA and RD, regardless of whether FW correction was applied, RD tended to be lower in the migraine group. We did not observe significant alterations in FW when comparing between groups, although FW tended to be lower in migraine patients. When comparing subject groups, a larger percentage of voxels presented significant differences when evaluating AD (both in TBSS and skeleton-ROI analyses – Table S-2).

ROI analysis

For FA values, we were unable to detect any common WM tracts with significant differences between groups in both diffusion models. We found a significantly higher FA value in the right superior cerebellar peduncle (SCP) (Fig. 2, A) in patients when using DTI. On the other hand, with FW-DTI, we obtained a significantly higher FA in the right corticospinal tract (CT) in controls. Although this WM tract presented a large effect size, none of these results survived correction for multiple comparisons (Table S-3).

For the remaining diffusion parameters (Fig. 2, B-D), both methods showed higher values in controls than in patients, and some WM tracts changes were common to both diffusion models.

For MD, the 7 common tracts were mainly projection fibers in the left hemisphere, while 20 tracts presented significant differences for only one of the diffusion signal models (11 DTI and 9 FW-DTI). Significant differences detected only with DTI were primarily in the left hemisphere, whereas those detected solely with FW-DTI were mainly in the right hemisphere, particularly in projection and association fibers.

Table 2 WM tracts where significantly decreased MD and AD values were found in the migraine patients compared to control subjects, considering the age of the subjects as a covariate. When using the DTI model, several regions presented a significant age effect, with decreasing MD and AD as age increased ('Negative age'). The total number of voxels and mean uncorrected p-value within each tract are shown for the MD and AD calculated from the original (DTI) and the corrected (FW-DTI) diffusion signals. R: Right, L: Left

	MD				AD					
	DTI		FW-DTI		DTI				FW-DTI	
	Negative age		Control > Migraine		Control > Migraine		Negative age		Control > Migraine	
JHU-WM atlas	**Voxels**	***p*-value**	**Voxels**	***p*-value**	**Voxels**	***p*-value**	**Voxels**	***p*-value**	**Voxels**	***p*-value**
Genu of corpus callosum					921	0.037			1062	0.021
Body of corpus callosum			275	0.044	1284	0.032			1160	0.022
Splenium of corpus callosum			647	0.043	1505	0.028			1400	0.024
Cerebral peduncle R					176	0.047				
Cerebral peduncle L					201	0.046			64	0.043
Anterior limb of internal capsule R					276	0.039			332	0.025
Anterior limb of internal capsule L	268	0.047			175	0.048			218	0.043
Posterior limb of internal capsule R					354	0.042			229	0.026
Posterior limb of internal capsule L	477	0.045			269	0.047	139	0.047	206	0.043
Retrolenticular part of internal capsule R			133	0.048	235	0.040			427	0.026
Retrolenticular part of internal capsule L	152	0.045			270	0.042			262	0.041
Anterior corona radiata R					782	0.037			978	0.024
Anterior corona radiata L	86	0.048			654	0.043	131	0.045	564	0.038
Superior corona radiata R					511	0.039			374	0.023
Superior corona radiata L	348	0.048	88	0.047	223	0.048			349	0.043
Posterior corona radiata R					177	0.035			193	0.036
Posterior corona radiata L					92	0.036			120	0.042
Posterior thalamic radiation R			386	0.046	491	0.033			612	0.023
Posterior thalamic radiation L					529	0.031			300	0.037
Sagittal stratum R									80	0.034
Sagittal stratum L					223	0.034			95	0.035
External capsule R					205	0.041			406	0.027
External capsule L	115	0.047	52	0.047	407	0.048			214	0.043
Cingulum (cingulate gyrus) L					192	0.039				
Cingulum (hippocampus) R									93	0.022
Fornix (cres) / Stria terminalis L					76	0.049				
Superior longitudinal fasciculus R			74	0.049	202	0.047			50	0.029
Superior longitudinal fasciculus L	306	0.047			454	0.044			332	0.044

Central
Right hemisphere
Left hemisphere

Regarding AD, there were 9 common tracts, mainly projection fibers (Figure S-3, B) and the CC (Figure S-4, B), 12 tracts with differences detected only by DTI, and 1 tract with changes identified solely by FW-DTI: the right retrolenticular part of IC.

Lastly, for RD significant differences between groups were found in the right SCP with both models (Table S-3).

On the other hand, the FW values also presented some significant differences with large effect sizes, located

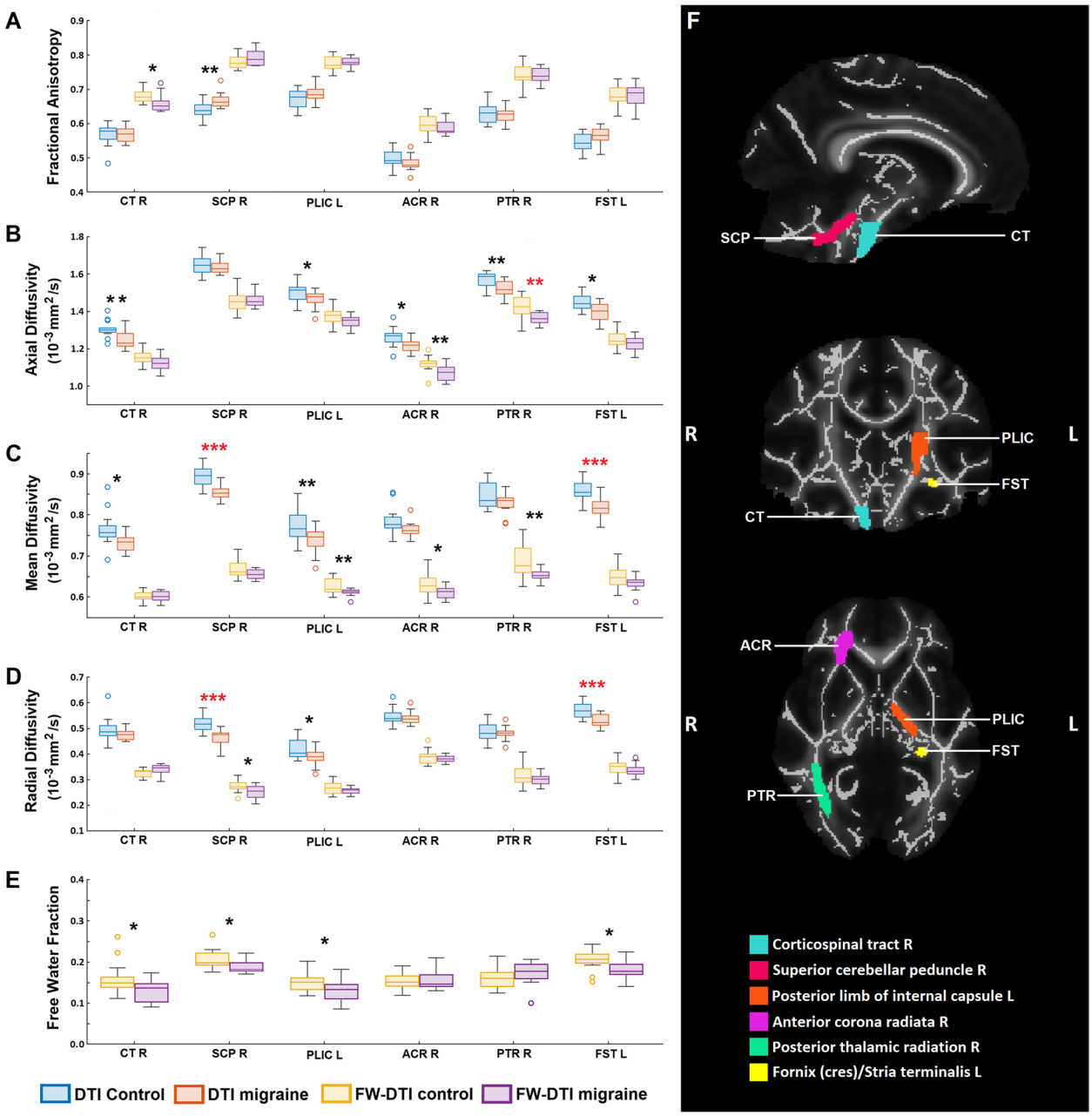

Fig. 2 WM tracts with significant differences in the diffusion parameters from the ROI analysis between migraine patients and control subjects, including age as a covariate. Skeletons were calculated from the diffusion parameters estimated from the original (DTI) and the corrected diffusion signals (FW-DTI). A: Fractional Anisotropy; B: Axial Diffusivity ($\times 10^{-3}$ mm^2/s); C: Mean Diffusivity ($\times 10^{-3}$ mm^2/s); D: Radial Diffusivity ($\times 10^{-3}$ mm^2/s); E: FW fraction; F: The ROIs used were retrieved from the JHU-WM atlas and shown in the standard space over the skeleton for improved visualization only (the intersections with the skeleton were used in the analysis instead). Blue: control subjects' parameters calculated from DTI; Red: migraine patients' parameters calculated from DTI; Yellow: control subjects' parameters calculated from FWDTI; Purple: migraine patients' parameters calculated from FWDTI. CT: corticospinal tract; SCP: superior cerebellar peduncle; PLIC: posterior limb of internal capsule; ACR: anterior corona radiata; PCR: posterior corona radiata; PTR: posterior thalamic radiation; CG: cingulum (cingulate gyrus); FST: fornix (cres)/stria terminalis. R: right hemisphere, L: left hemisphere. *$p < 0.05$, **$p < 0.01$, ***$p < 0.001$. In red, the significant differences that remain after multiple comparisons correction

in the right CT, SCP (Fig. 2, E), CG (Figure S-4, E) and superior CR; and the left CP, posterior CR (Figure S-3, E), posterior limb of IC and FST (Fig. 2, E).

Overall, we found more regions with significant differences in the parameters calculated from DTI than in those calculated with FW-DTI. For the MD calculated

from DTI, we identified 6 tracts where statistical significance remained after correction for multiple comparisons. Moreover, for the MD and RD from DTI, 2 WM tracts maintained their significance after the multiple comparison correction: the right SCP and the left FST, both with very large effect sizes.

When we consider the ROI analysis, the results differed from those of the TBSS voxelwise analysis. Significant differences in the MD values were found with DTI, and in 12 WM tracts with FW-DTI, which were not identified with the voxelwise analysis. On the other hand, with the ROI analysis, we could not detect several significant differences in MD and AD, with DTI and FW-DTI, that were detected in the voxelwise analysis. This was the case for some projection fibers (mainly AD for both mathematical approaches) or the body of the CC.

Furthermore, some tracts presented significant differences with both diffusion models (DTI and FW-DTI) and both analysis types (voxelwise and ROI). These tracts included the genu CC, right anterior CR and EC, and bilateral PTR for AD values. For MD, significant differences were found in left CP and superior CR, and bilateral posterior limb of IC. Significant differences in AD and MD were detected in the splenium CC and left anterior limb of IC.

Discussion

In this study, we report the effects of correction for FW in the analysis of dMRI data, when comparing episodic migraine patients to healthy controls. Voxelwise analysis of the WM skeleton revealed differences between the control and migraine groups, both with and without FW correction. Specifically, we found significantly lower AD values in migraine patients with both methods, while significantly lower MD values were detected only after applying FW correction. We did not detect significant differences in the FW fraction values, which tended to be lower in patients. The ROI analysis detected significant differences between groups for all diffusion parameters, calculated with either DTI or FW-DTI; besides the already-mentioned parameters, differences were found also for FA and RD, with significantly higher RD values in the control group. Nevertheless, the spatial pattern of detected WM alterations differed when using FW-DTI instead of standard DTI when comparing between patients and controls.

Decreased MD and AD values were obtained in previous studies in migraine patients [20, 21]. However, the results regarding RD alterations are inconsistent in the literature, with some studies showing higher values in migraine patients [37, 38], and no differences in others [20, 39]. For FA, most studies have described lower values in patients compared to controls [20, 39].

We found no previous studies on menstrual-related (episodic) migraine or to migraine in general that estimated the FW fraction. In this study, we found lower FW values in migraine patients, which could suggest cell swelling, also consistent with the observed decreases in the MD and AD values. Cell swelling processes may be caused by alterations in the osmotic balance between the extra- and intracellular spaces [40]. Since our data were extracted from the WM skeleton, our results would suggest that the swelling processes might affect the axonal membrane permeability. Indeed, the decreased FW and diffusivity values could be linked to a neurite beading process [41]. Moreover, WM is also constituted by astrocytes and microglia [42, 43]. These cells are responsible for brain homeostasis [44], and their proliferation and morphological changes are significant characteristics of inflammatory reactions. However, the diffusion parameters calculated from DTI and FW-DTI cannot distinguish which type of cells might be contributing more to the decreased diffusivity values, so the mechanisms behind the observed variations remain to be explained.

Migraine has been linked with inflammatory processes in previous studies [45]. Some investigations have tried to uncover the role played by cytokines in migraine [46], with higher levels of pro-inflammatory cytokines found during the ictal [47, 48] and interictal phases [49]. In contrast, investigations on anti-inflammatory cytokines levels presented diverse results, with studies indicating lower [50], unchanged [51] or higher [52] concentrations during the interictal phase. However, these studies used very different approaches for sample collection and analysis, and none were performed in menstrual-related migraine. Further studies need to be carried out on more homogenous patient groups with specific migraine types.

To investigate the role of inflammation in migraine patients compared to controls, we considered a diffusion model with two compartments: one characterized by isotropic FW diffusion [24] and the other corresponding to neuronal tissue, hypothesizing that neuroinflammation would impact the FW compartment more directly. After removing the FW contribution from the diffusion signal, the diffusion parameters were calculated with DTI (FW-DTI). This correction caused significantly lower MD, AD and RD values, as well as higher values of FA in both groups, consistent with previous studies using FW fitting methods different from the SM technique [53–56].

The FW fraction can also reflect tissue alterations due to pathology. We detected a few regions with significantly lower FW values in migraine patients in the ROI analysis. Normally, an increase in FW suggests an enlargement of the extracellular space [24, 57]. The decrease in the FW fraction of migraine patients might indicate a reduction in the extracellular space due to cellular and/or axonal

swelling. Nevertheless, although there was a tendency for lower FW values in migraine patients, as we could not detect generalized differences in the assessed WM tracts, this might indicate that no inflammation is present, or at least, that the biological processes during the interictal phase cause a zero net effect in the FW fraction compared to controls.

There were some tracts that exhibited significant differences for all diffusion models (DTI and FW-DTI) and analyses (voxelwise and ROI), strongly indicating that those tracts present alterations in menstrual-related episodic migraine patients. Alterations of the diffusion values in these brain regions have been reported in previous migraine studies [18]. The thalamus and cerebral cortex [58] are involved in the pathophysiology of migraine, and are connected through several projection tracts, such as IC or PTR, which presented significant changes in migraine patients [20, 59, 60]. Moreover, neurons from these projection tracts can modulate central signals from brain regions that participate in processes highly associated with migraine episodes [61]. In a prior study, the EC presented significant correlations between diffusion parameters and the onset of chronic migraine [19], and decreased AD values in migraine patients [39]. Previous studies in the CC, which is involved in the regulation of pain control, found lower MD and AD values in migraine patients [20, 39]. The CR is involved in motor functions [62, 63], reading [64] or mathematical competence [65], and lower AD values were detected in migraine patients [20].

In those tracts with significant differences in FW detected with ROI analysis, we observed significant alterations in diffusivity parameters when FW was significantly lower in patients. Most of those tracts presented significant differences with DTI but not with FW-DTI. We also detected alterations in the significance of tracts with no significant differences in FW when the correction was applied. This indicates that FW correction had an impact on the results. Some of the tracts that exhibited changes are related with migraine or pain modulation, and previous studies have also reported alterations in their diffusion parameters, as detailed below. The cingulum, which connects with the hippocampus, is related to cognitive control, executive function, and mild cognitive impairment. A study in cluster-headaches revealed lower AD in CgH [66]. The stria terminalis, or at least the bed nucleus, has been linked to pain mechanisms [67]. The retrolenticular part of the IC contains fibers from the optic system and is related to psychomotor impairment in depression [68]. A previous study had found alterations considering the duration of migraine as covariate [19], while another detected alterations in the diffusion parameters when considering new daily persistent headache [69]. The SS is involved in the processing of visual and language information; changes in this tract have been reported in a previous studies in episodic migraine patients with visual snow syndrome, and in another investigation related to neuropathic pain [67, 70]. Previous studies detected changes in the MCP, one considering migraine patients with epilepsy [71], and another migraine patients without aura [72].

On the other hand, the MD calculated with the DTI approach did not exhibit significant alterations in the voxelwise analysis. However, a negative age effect was detected in some WM tracts with MD values decreasing as the subject age increased. Previous studies with DTI have reported alterations in diffusion parameters due to the age of the subjects [73, 74], with a U-shape trajectory. Nevertheless, this was not the case when using the FW-DTI model. A previous study showed that the correction of the diffusion signal by extracting the FW fraction caused a flattening effect in MD values with age, compared with standard DTI [75].

Most of the significant differences that we detected exclusively with FW-DTI were in the right hemisphere. Previous investigations have studied hemispheric asymmetries, finding that this hemisphere is more related with emotion, attention [76] and pain [77]. Some MRI studies in migraine have also detected alterations predominantly in the right hemisphere using DTI, but comparing different types of migraine [37, 78]. This suggests that the alterations detected with DTI in other forms of migraine might also be present in this type of episodic migraine, without being detectable with the standard DTI model.

It is important to highlight that all previously mentioned migraine studies used DTI without correcting for FW. We do not expect this correction to invalidate the results from previous studies, but to improve specificity to the underlying pathological process of migraine. Indeed, brain tissue and FW have greatly different diffusion properties; if partial volume effects occur with a FW compartment having high isotropic diffusivity, the DTI approach will lead to an overestimation of the tissue's diffusivity parameters and to lower FA values. A large number of studies using DTI have pointed out that FW correction had a significant influence on the diffusion parameters, increasing sensitivity of MD and FA, and allowing for the detection of subtle alterations in WM microstructure [24, 54, 79]. Other studies have suggested that DTI analysis can be affected by multiple transient factors such as dehydration, stress or brain slice position, whose variability can lead to partial volume effects [54]. FW correction might reduce the impact of such factors on the results, which may explain the differences regarding the WM tracts where we found significant alterations with DTI and FW-DTI.

Along the study, we have detected differences between the skeleton voxelwise and the ROI analyses. These may be related not only to the different statistical analyses applied but also to the higher signal-to-noise ratio in the ROI analysis, due to the averaging effect across a larger number of voxels that could increase sensitivity to subtle differences in brain microstructure.

This study presents as its main limitations the low number of participants in both groups, and the non-uniform distribution of the data across age. A small sample size can present several disadvantages, from reduced statistical power (type II errors) to increased variability or limited generalizability, which may constrain our conclusions. However, this study focuses on a very specific type of episodic migraine, which allowed us to obtain a very homogeneous group of patients with specific and controlled features. This should decrease cross-subject variability compared to other migraine studies. Nonetheless, restricting the inclusion criteria limited patient recruitment possibilities and, in consequence, also the number of control subjects. On the other hand, the control group was younger than the migraine patients; although we included age as a covariate in our statistical analysis to minimize its impact, this may have affected our results.

Conclusion

This study showed that FW correction impacted the spatial pattern of WM alterations measured using dMRI in low-frequency episodic menstrual-related migraine patients without aura. Both DTI and FW-DTI models revealed significant differences in MD and AD when applying an ROI analysis, compatible with cellular swelling processes in WM tracts. Although the molecular mechanisms underlying the crosstalk between neurons and glial cells deserve further investigation, the correspondence between our results and previous studies done by other groups might indicate that different types of migraine suffer from similar biological processes. As the FW-DTI model may be too simplistic to capture these processes, further investigations with advanced methods are needed to confirm hypotheses related to inflammatory processes.

In conclusion, both DTI and FW-DTI models suggest abnormal WM properties in menstrual-related migraine patients, providing additional evidence to our understanding of this neurological disease, particularly in the context of menstrual-related migraine.

Abbreviations

CGRP	Calcitonin gene-related peptide
MRI	Magnetic resonance imaging
PET	Positron emission tomography
SPECT	Single-photon emission computed tomography
dMRI	Diffusion MRI
DTI	Diffusion tensor imaging
MD	Mean diffusivity
AD	Axial diffusivity
RD	Radial diffusivity
FA	Fractional anisotropy
WM	White matter
CC	Corpus callosum
CG	Cingulate gyrus
FW	Free-water
TR	Repetition time
TE	Echo time
SM	Spherical means
TBSS	Tract-based spatial statistics
FSL	FMRIB Software Library
ROI	Regions-of-interest
JHU-WM	Johns Hopkins University ICBM-DTI-81 WM
ANCOVA	Analysis of covariance
IC	Internal capsule
PTR	Posterior thalamic radiation
SLF	Superior longitudinal fasciculus
CR	Corona radiata
EC	External capsule
SS	Sagittal stratum
CP	Cerebral peduncle
FST	Fornix (cres)/stria terminalis
CgH	Cingulum (hippocampus)
SCP	Superior cerebellar peduncle
CT	Corticospinal tract
MCP	Middle cerebellar peduncle

Supplementary Information

The online version contains supplementary material available at https://doi.org/10.1186/s10194-025-01970-z.

Additional file 1.

Acknowledgements

We thank all the patients and healthy volunteers who agreed to take part in this study, as well as the radiographers who aided in the collection of the MRI data. We would like to thank Álvaro Planchuelo-Gómez for his methodological support and Antonio Tristán-Vega for the development of the spherical means technique software to calculate the free-water partial volume fraction.

Authors' contributions

IG: Formal analysis, Investigation, Visualization, Writing-original draft, Writing-review & editing. ARF: Data curation, Formal analysis, Investigation, Writing-review editing. ART: Data curation, Investigation, Methodology. IE: Data curation, Investigation, Methodology. GC: Data Curation, Investigation, Methodology. NAS: Methodology, Project administration, Resources. PV: Methodology, Resources. RGG: Conceptualization, Methodology, Project administration, Resources, Supervision. SAF: Conceptualization, Supervision, Writing-review & editing. PF: Conceptualization, Funding acquisition, Methodology, Project administration, Supervision, Writing-review & editing. RGN: Conceptualization, Methodology, Project administration, Supervision, Writing-review & editing.

Funding

This study was funded by the Portuguese Science Foundation (FCT) through grants SFRH/BD/139561/2018, COVID/BD/153268/2023, PTDC/EMD-EMD/29675/2017, LARSyS FCT funding (DOI: https://doi.org/10.54499/LA/P/0083/2020, https://doi.org/10.54499/UIDP/50009/2020, and https://doi.org/10.54499/UIDB/50009/2020), and Programa Operacional Regional de Lisboa 2020 LISBOA-01-0145-FEDER-029675. This work was also supported by Ministerio de Ciencia e Innovación PID2021-124407NB-I00 and TED2021-130758B-I00 funded by MCIN/AEI/10.13039/501100011033 and the European Union NextGenerationEU /PRTR. IG was supported by Margarita Salas grants CA1/RSUE/2021 – 00801 from Universidad Autónoma de Madrid, Ministerio de Universidades and Plan de Recuperación, Transformación y Resilencia (Spain).

Data availability
The data that supports the present results of this Research article are available from the corresponding author, upon reasonable request.

Declarations

Ethics approval and consent to participate
All experimental procedures were approved by the Health Ethics Commission of Hospital da Luz (CES/46/2018/ME) and conducted in compliance with the Declaration of Helsinki, Good Clinical Practice and all applicable regulations and laws. All subjects gave written informed consent.

Competing interests
The authors declare no conflict of interests. The authors declare that the research was conducted in the absence of any commercial or financial relationships that could be construed as a potential conflict of interest.

Author details
[1]Universidad Autónoma de Madrid, Madrid, Spain. [2]Institute for Systems and Robotics - Lisboa, Department of Bioengineering, Instituto Superior Técnico, Universidade de Lisboa, Lisbon, Portugal. [3]Laboratorio de Procesado de Imagen, Universidad de Valladolid, Valladolid, Spain. [4]Learning Health, Hospital da Luz, Lisbon, Portugal. [5]Imaging Department, Hospital da Luz, Lisbon, Portugal. [6]Neurology Department, Hospital da Luz, Lisbon, Portugal. [7]Center for Interdisciplinary Research in Health, Universidade Católica Portuguesa, Lisbon, Portugal.

Received: 26 August 2024 Accepted: 30 January 2025
Published online: 12 February 2025

References

1. Hoffmann J, Baca SM, Akerman S (2019) Neurovascular mechanisms of migraine and cluster headache. J Cereb Blood Flow Metab 39:573–594. https://doi.org/10.1177/0271678X17733655
2. (2018) Headache Classification Committee of the International Headache Society (IHS) The International Classification of Headache Disorders, 3rd edition. Cephalalgia 38:1–211. https://doi.org/10.1177/0333102417738202
3. Vetvik KG, MacGregor EA (2021) Menstrual migraine: a distinct disorder needing greater recognition. Lancet Neurol 20:304–315. https://doi.org/10.1016/S1474-4422(20)30482-8
4. Todd C, Lagman-Bartolome AM, Lay C (2018) Women and migraine: the role of hormones. Curr Neurol Neurosci Rep 18:42. https://doi.org/10.1007/s11910-018-0845-3
5. Olesen J, Burstein R, Ashina M, Tfelt-Hansen P (2009) Origin of pain in migraine: evidence for peripheral sensitisation. Lancet Neurol 8:679–690. https://doi.org/10.1016/S1474-4422(09)70090-0
6. Pietrobon D, Moskowitz MA (2013) Pathophysiology of Migraine. Annu Rev Physiol 75:365–391. https://doi.org/10.1146/annurev-physiol-030212-183717
7. Bianca Raffaelli E, Storch LH, Overeem et al (2023) Sex hormones and calcitonin gene–related peptide in Women with Migraine. Neurology 100:e1825. https://doi.org/10.1212/WNL.0000000000207114
8. Krause DN, Warfvinge K, Haanes KA, Edvinsson L (2021) Hormonal influences in migraine — interactions of oestrogen, oxytocin and CGRP. Nat Reviews Neurol 17:621–633. https://doi.org/10.1038/s41582-021-00544-2
9. Labastida-Ramírez A, Rubio-Beltrán E, Villalón CM, MaassenVanDenBrink A (2019) Gender aspects of CGRP in migraine. Cephalalgia 39:435–444. https://doi.org/10.1177/0333102417739584
10. Messina R, Rocca MA, Goadsby PJ, Filippi M (2023) Insights into migraine attacks from neuroimaging. Lancet Neurol 22:834–846. https://doi.org/10.1016/S1474-4422(23)00152-7
11. Schwedt TJ, Chiang C-C, Chong CD, Dodick DW (2015) Functional MRI of migraine. Lancet Neurol 14:81–91. https://doi.org/10.1016/S1474-4422(14)70193-0
12. Ashina M, Terwindt GM, Al-Karagholi MA-M et al (2021) Migraine: disease characterisation, biomarkers, and precision medicine. Lancet 397:1496–1504. https://doi.org/10.1016/S0140-6736(20)32162-0
13. Wang Z-w, Yin Z-h, Wang X, Zhang Y-t, Xu T, Du J-r, Wen Y, Liao H-q, Zhao Y, Liang F-r, Zhao L (2022) Brain structural and functional changes during menstrual migraine: relationships with pain. Front Mol Neurosci 15:967103. https://doi.org/10.3389/fnmol.2022.967103
14. Li X, Khan A, Li Y et al (2021) Hyperconnection and hyperperfusion of overlapping brain regions in patients with menstrual-related migraine: a multimodal neuroimaging study. Neuroradiology 63:741–749. https://doi.org/10.1007/s00234-020-02623-5
15. Zhang Y, Xu T, Wang Z et al (2021) Differences in topological properties of functional brain networks between menstrually-related and non-menstrual migraine without aura. Brain Imaging Behav 15:1450–1459. https://doi.org/10.1007/s11682-020-00344-0
16. Xu T, Zhang Y, Wang C et al (2020) Brain structural and functional differences between pure menstrual migraine and menstrually-related migraine. Sci Rep 10:16454. https://doi.org/10.1038/s41598-020-73399-0
17. Le Bihan D, Mangin J-F, Poupon C et al (2001) Diffusion tensor imaging: concepts and applications. J Magn Reson Imaging 13:534–546. https://doi.org/10.1002/jmri.1076
18. Rahimi R, Dolatshahi M, Abbasi-Feijani F et al (2022) Microstructural white matter alterations associated with migraine headaches: a systematic review of diffusion tensor imaging studies. Brain Imaging Behav 16:2375–2401. https://doi.org/10.1007/s11682-022-00690-1
19. Planchuelo-Gómez Á, García-Azorín D, Guerrero ÁL et al (2020) White matter changes in chronic and episodic migraine: a diffusion tensor imaging study. J Headache Pain 21:1. https://doi.org/10.1186/s10194-019-1071-3
20. Yu D, Yuan K, Qin W et al (2013) Axonal loss of white matter in migraine without aura: a tract-based spatial statistics study. Cephalalgia 33:34–42. https://doi.org/10.1177/0333102412466964
21. Rocca MA, Colombo B, Inglese M et al (2003) A diffusion tensor magnetic resonance imaging study of brain tissue from patients with migraine. J Neurol Neurosurg Psychiatry 74:501. https://doi.org/10.1136/jnnp.74.4.501
22. Fouto AR, Nunes RG, Guadilla I et al (2023) Episodic menstrual migraine patients exhibit white matter microstructural changes compared to hormonal controls. In: Proceedings of the International Society for Magnetic Resonance in Medicine, Scientific Meeting and Exhibition. Toronto, Canada, p 2639. https://doi.org/10.58530/2023/2639
23. Edvinsson L, Haanes KA, Warfvinge K (2019) Does inflammation have a role in migraine? Nat Reviews Neurol 15:483–490. https://doi.org/10.1038/s41582-019-0216-y
24. Pasternak O, Sochen N, Gur Y et al (2009) Free water elimination and mapping from diffusion MRI. Magn Reson Med 62:717–730. https://doi.org/10.1002/mrm.22055
25. Ofer Pasternak C-F, Westin S, Bouix et al (2012) Excessive extracellular volume reveals a neurodegenerative pattern in Schizophrenia Onset. J Neurosci 32:17365. https://doi.org/10.1523/JNEUROSCI.2904-12.2012
26. Ji F, Pasternak O, Liu S et al (2017) Distinct white matter microstructural abnormalities and extracellular water increases relate to cognitive impairment in Alzheimer's disease with and without cerebrovascular disease. Alzheimer's Res Therapy 9:63. https://doi.org/10.1186/s13195-017-0292-4
27. Fouto AR, Henriques RN, Golub M et al (2024) Impact of truncating diffusion MRI scans on diffusional kurtosis imaging. Magnetic Resonance Materials in Physics, Biology and Medicine. https://doi.org/10.1007/s10334-024-01153-y
28. Domingos C, Fouto AR, Nunes RG et al (2023) Impact of susceptibility-induced distortion correction on perfusion imaging by pCASL with a segmented 3D GRASE readout. Magn Reson Imaging 102:141–150. https://doi.org/10.1016/j.mri.2023.06.010
29. Ruiz-Tagle A, Figueiredo P, Pinto J et al (2024) Working memory during spontaneous migraine attacks: an fMRI study. Neurol Sci 45:1201–1208. https://doi.org/10.1007/s10072-023-07120-0
30. Ades-Aron B, Veraart J, Kochunov P et al (2018) Evaluation of the accuracy and precision of the diffusion parameter EStImation with Gibbs and NoisE removal pipeline. NeuroImage 183:532–543. https://doi.org/10.1016/j.neuroimage.2018.07.066
31. Tristán-Vega A, París G, de Luis-García R, Aja-Fernández S (2022) Accurate free-water estimation in white matter from fast diffusion MRI acquisitions using the spherical means technique. Magn Reson Med 87:1028–1035. https://doi.org/10.1002/mrm.28997
32. Pierpaoli C, Jones DK (2004) Removing CSF Contamination in Brain DT-MRIs by Using a Two-Compartment Tensor Model. In: Proceedings

International Society for Magnetic Resonance in Medicine. Melbourne, Australia, p 1215
33. Chang L-C, Jones DK, Pierpaoli C (2005) RESTORE: robust estimation of tensors by outlier rejection. Magn Reson Med 53:1088–1095. https://doi.org/10.1002/mrm.20426
34. Smith SM, Jenkinson M, Johansen-Berg H et al (2006) Tract-based spatial statistics: Voxelwise analysis of multi-subject diffusion data. NeuroImage 31:1487–1505. https://doi.org/10.1016/j.neuroimage.2006.02.024
35. Oishi K, Zilles K, Amunts K et al (2008) Human brain white matter atlas: identification and assignment of common anatomical structures in superficial white matter. NeuroImage 43:447–457. https://doi.org/10.1016/j.neuroimage.2008.07.009
36. Winkler AM, Ridgway GR, Webster MA et al (2014) Permutation inference for the general linear model. NeuroImage 92:381–397. https://doi.org/10.1016/j.neuroimage.2014.01.060
37. Planchuelo-Gómez Á, García-Azorín D, Guerrero ÁL et al (2023) Structural brain changes in patients with persistent headache after COVID-19 resolution. J Neurol 270:13–31. https://doi.org/10.1007/s00415-022-11398-z
38. Shibata Y, Ishiyama S, Matsushita A (2018) White matter diffusion abnormalities in migraine and medication overuse headache: a 1.5-T tract-based spatial statistics study. Clin Neurol Neurosurg 174:167–173. https://doi.org/10.1016/j.clineuro.2018.09.022
39. Yu D, Yuan K, Zhao L et al (2013) White matter integrity affected by depressive symptoms in migraine without aura: a tract-based spatial statistics study. NMR Biomed 26:1103–1112. https://doi.org/10.1002/nbm.2924
40. Le Bihan D (2007) The 'wet mind': water and functional neuroimaging. Phys Med Biol 52:R57. https://doi.org/10.1088/0031-9155/52/7/R02
41. Budde MD, Frank JA (2010) Neurite beading is sufficient to decrease the apparent diffusion coefficient after ischemic stroke. Proc Natl Acad Sci 107:14472–14477. https://doi.org/10.1073/pnas.1004841107
42. Sofroniew MV (2020) Astrocyte reactivity: subtypes, States, and functions in CNS innate immunity. Trends Immunol 41:758–770. https://doi.org/10.1016/j.it.2020.07.004
43. Amor S, McNamara NB, Gerrits E et al (2022) White matter microglia heterogeneity in the CNS. Acta Neuropathol 143:125–141. https://doi.org/10.1007/s00401-021-02389-x
44. Verkhratsky A, Nedergaard M (2018) Physiology of Astroglia. Physiol Rev 98:239–389. https://doi.org/10.1152/physrev.00042.2016
45. Christensen RH, Gollion C, Amin FM et al (2022) Imaging the inflammatory phenotype in migraine. J Headache Pain 23:60. https://doi.org/10.1186/s10194-022-01430-y
46. Thuraiaiyah J, Erritzøe-Jervild M, Al-Khazali HM et al (2022) The role of cytokines in migraine: a systematic review. Cephalalgia 42:1565–1588. https://doi.org/10.1177/03331024221118924
47. Perini F, D'Andrea G, Galloni E, et al et al (2005) Plasma cytokine levels in migraineurs and controls. Headache: J Head Face Pain 45:926–931. https://doi.org/10.1111/j.1526-4610.2005.05135.x
48. Sarchielli P, Alberti A, Baldi A et al (2006) Proinflammatory cytokines, adhesion molecules, and lymphocyte integrin expression in the Internal Jugular blood of Migraine patients without Aura Assessed Ictally. Headache: J Head Face Pain 46:200–207. https://doi.org/10.1111/j.1526-4610.2006.00337.x
49. Uzar E, Evliyaoğlu O, Yucel Y et al (2011) Serum cytokine and pro-brain natriuretic peptide (BNP) levels in patients with migraine. Eur Rev Med Pharmacol Sci 15:1111–1116
50. Oliveira AB, Bachi ALL, Ribeiro RT et al (2017) Unbalanced plasma TNF-α and IL-12/IL-10 profile in women with migraine is associated with psychological and physiological outcomes. J Neuroimmunol 313:138–144. https://doi.org/10.1016/j.jneuroim.2017.09.008
51. Fidan I, Yüksel S, Ýmir T et al (2006) The importance of cytokines, chemokines and nitric oxide in pathophysiology of migraine. J Neuroimmunol 171:184–188. https://doi.org/10.1016/j.jneuroim.2005.10.005
52. Chaudhry SR, Lendvai IS, Muhammad S et al (2019) Inter-ictal assay of peripheral circulating inflammatory mediators in migraine patients under adjunctive cervical non-invasive vagus nerve stimulation (nVNS): a proof-of-concept study. Brain Stimul 12:643–651. https://doi.org/10.1016/j.brs.2019.01.008
53. Hoy AR, Koay CG, Kecskemeti SR, Alexander AL (2014) Optimization of a free water elimination two-compartment model for diffusion tensor imaging. NeuroImage 103:323–333. https://doi.org/10.1016/j.neuroimage.2014.09.053
54. Albi A, Pasternak O, Minati L et al (2017) Free water elimination improves test–retest reproducibility of diffusion tensor imaging indices in the brain: a longitudinal multisite study of healthy elderly subjects. Hum Brain Mapp 38:12–26. https://doi.org/10.1002/hbm.23350
55. Edde M, Theaud G, Rheault F et al (2020) Free water: a marker of age-related modifications of the cingulum white matter and its association with cognitive decline. PLoS ONE 15:e0242696. https://doi.org/10.1371/journal.pone.0242696
56. Hoy AR, Kecskemeti SR, Alexander AL (2015) Free water elimination diffusion tractography: a comparison with conventional and fluid-attenuated inversion recovery, diffusion tensor imaging acquisitions. J Magn Reson Imaging 42:1572–1581. https://doi.org/10.1002/jmri.24925
57. Wu D, Wu Q, Li F et al (2024) Free water alterations in different inflammatory subgroups in schizophrenia. Brain Behav Immun 115:557–564. https://doi.org/10.1016/j.bbi.2023.11.006
58. Younis S, Hougaard A, Noseda R, Ashina M (2019) Current understanding of thalamic structure and function in migraine. Cephalalgia 39:1675–1682. https://doi.org/10.1177/0333102418791595
59. Coppola G, Tinelli E, Lepre C et al (2014) Dynamic changes in thalamic microstructure of migraine without aura patients: a diffusion tensor magnetic resonance imaging study. Eur J Neurol 21:287–e13. https://doi.org/10.1111/ene.12296
60. May A (2009) New insights into headache: an update on functional and structural imaging findings. Nat Reviews Neurol 5:199–209. https://doi.org/10.1038/nrneurol.2009.28
61. Dodick DW (2018) Migraine. Lancet 391:1315–1330. https://doi.org/10.1016/S0140-6736(18)30478-1
62. Shelton F, de NAP, Reding MJ (2001) Effect of Lesion Location on Upper Limb Motor Recovery after Stroke. Stroke 32:107–112. https://doi.org/10.1161/01.STR.32.1.107
63. Jong S, Kim A, Pope (2005) Somatotopically located motor fibers in corona radiata: evidence from subcortical small infarcts. Neurology 64:1438. https://doi.org/10.1212/01.WNL.0000158656.09335.E7
64. Vandermosten M, Boets B, Wouters J, Ghesquière P (2012) A qualitative and quantitative review of diffusion tensor imaging studies in reading and dyslexia. Neurosci Biobehavioral Reviews 36:1532–1552. https://doi.org/10.1016/j.neubiorev.2012.04.002
65. van Eimeren L, Grabner RH, Koschutnig K et al (2010) Structure-function relationships underlying calculation: a combined diffusion tensor imaging and fMRI study. NeuroImage 52:358–363. https://doi.org/10.1016/j.neuroimage.2010.04.001
66. Chou K-H, Yang F-C, Fuh J-L et al (2014) Altered white matter microstructural connectivity in cluster headaches: a longitudinal diffusion tensor imaging study. Cephalalgia 34:1040–1052. https://doi.org/10.1177/0333102414527649
67. Dong D, Hosomi K, Mori N et al. White matter microstructural alterations in patients with neuropathic pain after spinal cord injury: a diffusion tensor imaging study. Front Neurol, 2023:14
68. Hyett MP, Perry A, Breakspear M et al (2018) White matter alterations in the internal capsule and psychomotor impairment in melancholic depression. PLoS ONE 13:e0195672. https://doi.org/10.1371/journal.pone.0195672
69. Mei Y, Wang W, Qiu D et al (2023) Micro-structural white matter abnormalities in new daily persistent headache: a DTI study using TBSS analysis. J Headache Pain 24:80. https://doi.org/10.1186/s10194-023-01620-2
70. Michels L, Stämpfli P, Aldusary N et al. Widespread white matter alterations in patients with visual Snow Syndrome. Front Neurol. 2021:12
71. Huang Q, Lv X, He Y et al (2017) Structural differences in interictal migraine attack after epilepsy: a diffusion tensor imaging analysis. Epilepsy Behav 77:8–12. https://doi.org/10.1016/j.yebeh.2017.09.002
72. Qin Z, He X-W, Zhang J et al (2019) Structural changes of cerebellum and brainstem in migraine without aura. J Headache Pain 20:93. https://doi.org/10.1186/s10194-019-1045-5
73. Westlye LT, Walhovd KB, Dale AM et al (2010) Life-span changes of the human brain White Matter: Diffusion Tensor Imaging (DTI) and Volumetry. Cereb Cortex 20:2055–2068. https://doi.org/10.1093/cercor/bhp280
74. Beck D, de Lange A-MG, Maximov II et al (2021) White matter microstructure across the adult lifespan: a mixed longitudinal and cross-sectional

study using advanced diffusion models and brain-age prediction. NeuroImage 224:117441. https://doi.org/10.1016/j.neuroimage.2020.117441
75. Pieciak T, París G, Beck D et al (2023) Spherical means-based free-water volume fraction from diffusion MRI increases non-linearly with age in the white matter of the healthy human brain. NeuroImage 279:120324. https://doi.org/10.1016/j.neuroimage.2023.120324
76. Hartikainen KM (2021) Emotion-attention Interaction in the right hemisphere. https://doi.org/10.3390/brainsci11081006. Brain Sciences 11:
77. Hecht D (2010) Depression and the hyperactive right-hemisphere. Neurosci Res 68:77–87. https://doi.org/10.1016/j.neures.2010.06.013
78. Gomez-Beldarrain M, Oroz I, Zapirain BG et al (2016) Right fronto-insular white matter tracts link cognitive reserve and pain in migraine patients. J Headache Pain 17:4. https://doi.org/10.1186/s10194-016-0593-1
79. Bergamino M, Walsh RR, Stokes AM (2021) Free-water diffusion tensor imaging improves the accuracy and sensitivity of white matter analysis in Alzheimer's disease. Sci Rep 11:6990. https://doi.org/10.1038/s41598-021-86505-7

Publisher's Note